

## RESEARCH ARTICLE

# The impact of Bismuth Ion on the physical and optical characteristics of borate glasses

Bhupendra Patankar<sup>1</sup>, Ghizal F. Ansari<sup>1,\*</sup>, Sukhdev Bairagi<sup>2</sup>

<sup>1</sup> Department of Physics, Madhyaanchal Professional University, Bhopal-462044, India

<sup>2</sup> Department of Physics, Sardar Vallabhbhai Patel Govt. College Nalkheda-465445, India

\* Corresponding author: Ghizal F. Ansari, ansarigf@rediffmail.com

### ABSTRACT

The bismuth doped borate ( $\text{Bi}_2\text{O}_3\text{-B}_2\text{O}_3$ ) glasses were made using the melt quench process. The physico-optical characteristics, including their molar and density of the specimens were examined. The density readings were obtained using the Archimedes principle. The X-Ray diffraction was used to verify that the specimens are amorphous. Using Tauc's approach, the optical characteristics of the specimens, including their direct and indirect forbidden energy gaps, were computed. The Urbach energy and steepness of the glass system were calculated to determine its disorderliness. The effect of Bi on physical and optical properties as density, polaron radius, forbidden energy gap, refractive index etc, were observed. The metallization criteria were used to examine the materials' non-metallic character.

**Keywords:** borate glass; tauc's plot; urbach energy; forbidden energy gap

## 1. Introduction

The potential uses of borate base glasses including heavy metal oxides (HMO) as lightning phosphors, lasing host material and other photonic devices have sparked particular interest<sup>[1-2]</sup>. Applications for heavy metal oxide doped borate glasses include surgical lasers, shields glasses, and their glass-ceramic counterparts. They are also used in optical fibres and optoelectronic devices<sup>[3-5]</sup>. Stable glasses containing heavy metal and second group metal oxides are formed by boric acid ( $\text{H}_3\text{BO}_3$ ). The rare-earth ion are found to soluble in the with HMO dope borate glasses. Glasses containing PbO have a low glass transition temperature and a high refractive index<sup>[6]</sup>. Electronic polarizability is a critical component in the usage of glasses as optical and electrical materials. The electrical polarizability of the components in the glass matrix determines the non-linear response to incoming radiation that glassy materials display. Conditional glass modifiers, such as ZnO, TeO<sub>2</sub>, PbO, and Bi<sub>2</sub>O<sub>3</sub>, can be added to oxide materials that produce glass, such as B<sub>2</sub>O<sub>3</sub>, SiO<sub>2</sub>, GeO<sub>2</sub>, P<sub>2</sub>O<sub>5</sub>, and As<sub>2</sub>O<sub>3</sub>, to improve their capacity to form glass, stability, and chemical durability.

Glasses made of bismuth borate are a potential family of materials for use in modern technology. For more than two decades, the field of photonics was involved in most of these applications<sup>[7-15]</sup>. Transparent glassy sample with a prominent refractive index have been proposed as viable substitutes for semiconductor materials with nonlinear optical characteristics in earlier research<sup>[16]</sup>. Therefore, it is desired to have stable

#### ARTICLE INFO

Received: 14 May 2024 | Accepted: 10 July 2024 | Available online: 23 July 2024

#### CITATION

Patankar B, Ansari GF, Bairagi S. The impact of Bismuth Ion on the physical and optical characteristics of borate glasses. *Micromaterials and Interfaces* 2024; 2(1): 6289. doi: 10.59429/mi.v2i1.6289

#### COPYRIGHT

Copyright © 2024 by author(s). *Micromaterials and Interfaces* is published by Arts and Science Press Pte. Ltd. This is an Open Access article distributed under the terms of the Creative Commons Attribution License (<https://creativecommons.org/licenses/by/4.0/>), permitting distribution and reproduction in any medium, provided the original work is cited.

glass samples with a wide forming range that contain highly polarizable metal ions; the bismuth-borate system is one such system. By using the twin roller quenching approach, present works on glass formation and characteristics in the  $\text{Bi}_2\text{O}_3\text{-B}_2\text{O}_3$  system have expanded the glass forming range up to about 88.2 mol%  $\text{Bi}_2\text{O}_3$ . The distinctive linear and nonlinear optical characteristics of glasses  $x\text{Bi}_2\text{O}_3\text{-(1-x)}\text{B}_2\text{O}_3$  that may be adjusted by changing the  $\text{Bi}_2\text{O}_3$  concentration throughout a wide composition range are the main reason for their continued popularity [17-19].

Different concentrations of  $\text{Bi}_2\text{O}_3$  have been synthesized into glasses of bismuth borate. Properties, both optical and physical, were computed. Studies have been conducted on the impact of Bi on physical and optical characteristics.

## 2. Experimental techniques

The traditional melt and quench procedure is used to create glass systems with the composition  $\text{B}_2\text{O}_3\text{-Bi}_2\text{O}_3\text{-Na}_2\text{O}$  in the mole percent ratio  $(90-x) \% : x \% : 10\%$ , where  $x$  is specified as 5, 10, 15, and 20%. Each component of the batch composition is mole-percentage weighed using an electronic machine and thoroughly mixed using a mortar and pestle. The batch mixture is placed in an alumina crucible and heated to a temperature of  $960^\circ\text{C}$  using an electrical furnace. To achieve homogeneity, the mixture is melted for thirty to forty minutes while being shook constantly. Using a steel rod, the melt was rapidly poured over a hot stainless steel plate that had been kept at  $250^\circ\text{C}$ . For two hours, the new samples are annealed at  $250^\circ\text{C}$  to release internal tensions. Glass pellets with a radius of 2.5-3.5 mm and a width of 2-3 mm are created, devoid of bubbles. The resulting glasses, known as BBN1, BBN2, BBN3, and BBN4, are clear, translucent, and have a little yellowish hue. The samples' density was calculated by using the Archimedes principle, and other physical characteristics such as the concentration of Bi-ions, the oxygen packed density (OPD) in the samples, the inter-ionic distance, and the polaron radius were computed. Samples with optical characteristics were then used in optical absorption tests. The Research India model no. RI2SA spectrometer records the optical absorption spectra between 250 and 1100 nm at room temperature. The refractive index values of the glass samples are determined using the forbidden energy gap ( $E_{op}$ ) measurements.

## 3. Results and discussion

### 3.1. Physical properties

#### 3.1.1. XRD

The X-Ray diffractogram of the synthesized glasses using a Rigaku Smart Lab 9kW at room temperature are shown in **Figure 1**. The plot is flat with a broad hump between  $25$  and  $35^\circ$  and no sharp peak, and hence prepared samples are noncrystalline (amorphous).

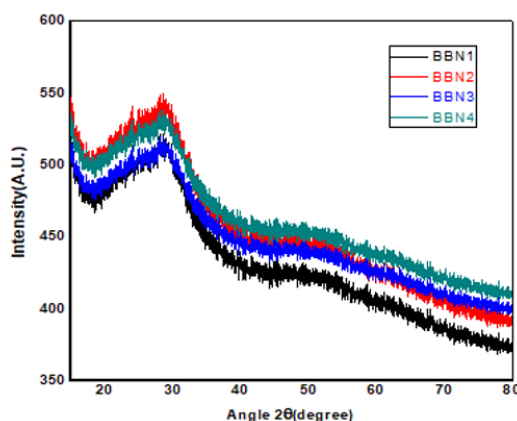


**Figure 1.** X-Ray Diffractogram of BBN glasses.

### 3.1.2. Density ( $\rho$ ) and Molar Volume ( $V_M$ )

Density ( $\rho$ ) and molar volume ( $V_M$ ) are important physical identity to investigate. Equation (1) was used to calculate the density measurements of the manufactured samples using Archimedes' principle<sup>[20-21]</sup>:

$$\rho = \left( \frac{W_a}{W_a - W_l} \right) \rho_1 \quad (1)$$

where  $W_a$  and  $W_l$  are the weight of specimens in air and in liquid, and  $\rho_1$  is the density of distilled water that is used as an immersion fluid. To obtain an accurate measurement, the weight of the samples was measured using an electronic balance. Equation (2) was used to determine the molar volume ( $V_M$ ) based on the samples' molecular weight and density<sup>[20-21]</sup>:

$$V_M = \frac{M}{\rho} \quad (2)$$

where  $m$  stands for the samples' molecular weight.

**Table 1** consists of the glass composition as well as the created samples' molar mass, density, and molar volume values. The glass's density increases with its  $\text{Bi}_2\text{O}_3$  content, which varies between 4.248 and 4.542  $\text{g cm}^{-3}$ . The molecular weight ( $M$ ) of  $\text{Bi}_2\text{O}_3$  is responsible for the increase in glass density. Molar volume exhibits an inverse relationship with density and decreases as  $\text{Bi}_2\text{O}_3$  content increases. The decrease in the bond length or inter-atom spacing of the glass network is responsible for the decrease in molar volume<sup>[22]</sup>. **Figure 2** shows how the density and molar volume change as the percentage share of bismuth oxide mol in BBN glasses increases.

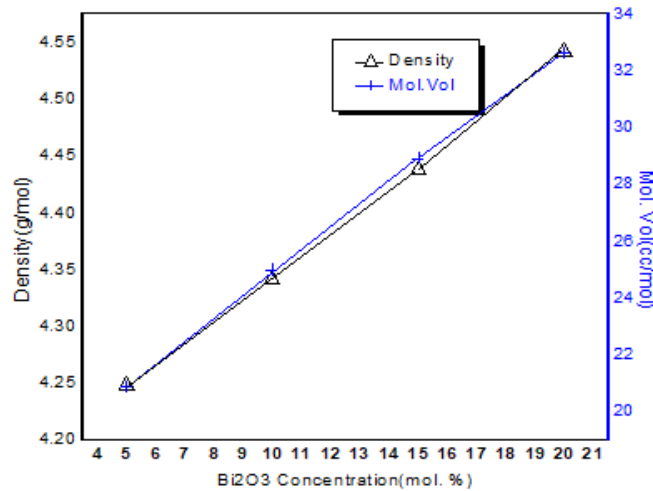


**Figure 2.** Variation in density and molar volume with change in  $\text{Bi}_2\text{O}_3$  concentration.

### 3.1.3. Inter-nuclear distance, concentration, field strength and polaron radius

The following formulas were used to determine the molar volume of boron ( $V_{m(B)}$ ) and the average B-B distance ( $d_{(B-B)}$ ), respectively.<sup>[23]</sup>:

$$V_{m(B)} = V_m \div [2(1 - X_B)] \quad (3)$$

$$d_{(B-B)} = [V_{m(B)} \div NA]^{1/3} \quad (4)$$

where  $V_{m(B)}$ ,  $X_B$ ,  $NA$  and  $N_{Bi}$  represent molar volume boron molar fraction, and Avogadro's number. Further

Bi<sub>2</sub>O<sub>3</sub> concentration (N<sub>Bi</sub>) and inter-nuclear distance (Ri) in the glass system can be studied by equation, polaron radius (Rp) and field strength (F) were calculated as <sup>[20-21]</sup>:

$$Ri = (1 \div N_{Bi})^{1/3} \quad (5)$$

$$N_{Bi} = [(X_{Bi} \times NA \times \rho) \div M] \quad (6)$$

$$Rp = (1/2)(\pi/6N_{Bi})^{1/3} \quad (7)$$

where X<sub>Bi</sub> molar fraction of Bi, M is molecular weight of the glass. The field strength (F) have been calculated by using equations following equations

$$F = (Z \div Rp^2) \quad (8)$$

where Z is the valence of Bi ion. By using equation (12), The oxygen packing density (OPD) is one crucial measure to look at the tightness and compactness of the oxide network in the prepared glasses, evaluated by following relation <sup>[20-21]</sup>:

$$OPD = (1000 \times No) \div Vm \quad (9)$$

The evaluated values molar volume, volume of boron and average B-B distance, Bi<sub>2</sub>O<sub>3</sub> concentration, inter-nuclear distance, polaron radius, field strength and OPD for the synthesized glasses are shown in **Table 1**.

**Table 1.** Physical properties of BBN glasses.

Specimen	BBN1	BBN2	BBN3	BBN4
Batch Composition	85% B <sub>2</sub> O <sub>3</sub> - 5% Bi <sub>2</sub> O <sub>3</sub> - 10% Na <sub>2</sub> O	80% B <sub>2</sub> O <sub>3</sub> - 10% Bi <sub>2</sub> O <sub>3</sub> - 10% Na <sub>2</sub> O	75% B <sub>2</sub> O <sub>3</sub> - 15% Bi <sub>2</sub> O <sub>3</sub> - 10% Na <sub>2</sub> O	70% B <sub>2</sub> O <sub>3</sub> - 20% Bi <sub>2</sub> O <sub>3</sub> - 10% Na <sub>2</sub> O
Molar Mass M - (g.mol <sup>-1</sup> )	88.66	108.48	128.3	148.12
Molar Volume V <sub>m</sub> -(cc.mol <sup>-1</sup> )	20.871	24.98388	28.90942	32.60678
Density ρ (gm/cc)	4.248	4.342	4.438	4.542
molar volume of boron V <sub>m(B)</sub> - (cc.mol <sup>-1</sup> )	82.45908	72.80537	66.54564	61.98008
B-B distance d <sub>(B-B)-A°</sub>	6.095	5.850	5.679	5.547
Bi ion concentration (N <sub>Bi</sub> )(× 10 <sup>3</sup> /cc)	1.217	2.068	2.715	3.239
inter-nuclear distance (Ri)- x 10 <sup>8</sup> cm	2.01771	1.6909	1.5442	1.4561
polaron radius (Rp)- x 10 <sup>9</sup> cm	5.637	4.7241	4.3143	4.0679
field strength(F)(× 10 <sup>16</sup> cm <sup>-2</sup> )	9.4411	13.4422E	16.1171	18.1288
OPD	113.1876	96.14691	84.15282	75.29311

## 3.2. Optical properties

### 3.2.1. Forbidden energy gaps and urbach's energy

The glass samples' optical absorption spectra are shown in **Figure 3**. It is clear from Figure that specimen exhibit low absorption. This is what makes samples of amorphous glass unique. The glass sample absorbs

incident light according to the well-known Beer-Lambert-Bouguer law.

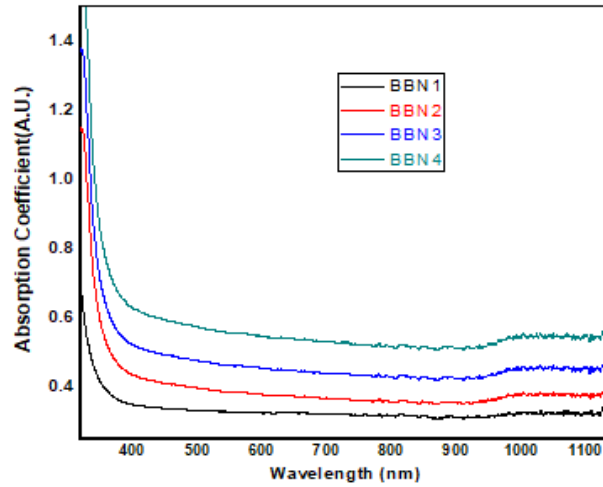


Figure 3. Optical Absorption spectra of BBN glasses.

The following relation can be used to calculate the optical absorption coefficient  $\alpha(\nu)$  of a glass sample of thickness  $\tau$  in the near absorption edge.

$$\alpha(\nu) = \frac{1}{\tau} \ln \frac{I_0}{I_t} \quad (10)$$

where  $\ln(I_0/I_t)$  is the absorbance,  $I_0$  and  $I_t$  are the intensities of incident and transmitted light respectively. The optical energy band gaps can be determined by Tauc's rule <sup>[24]</sup>

$$\alpha(\nu) = \frac{c}{h\nu} (h\nu - E_{op})^n \quad (11)$$

where "n" can have values of  $\frac{1}{2}$  and 2, which stand for direct prohibited and indirect permissible transitions, respectively, and c is a constant. In this case,  $h\nu$  is the incident photon energy and  $E_{op}$  is the forbidden energy gap. The glass sample Tauc's plots are displayed in **Figures 4 and 5**.

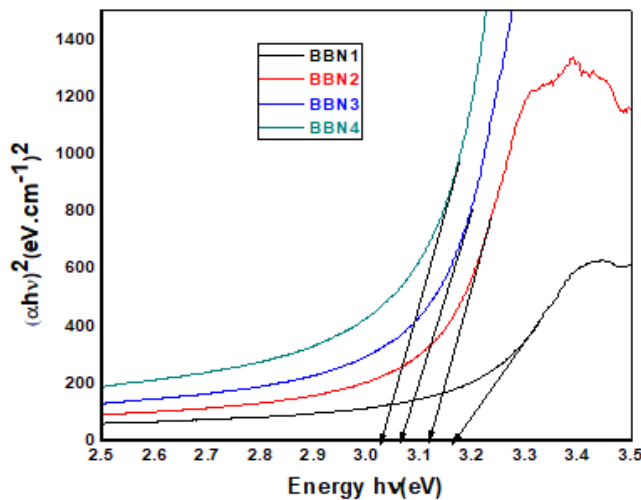
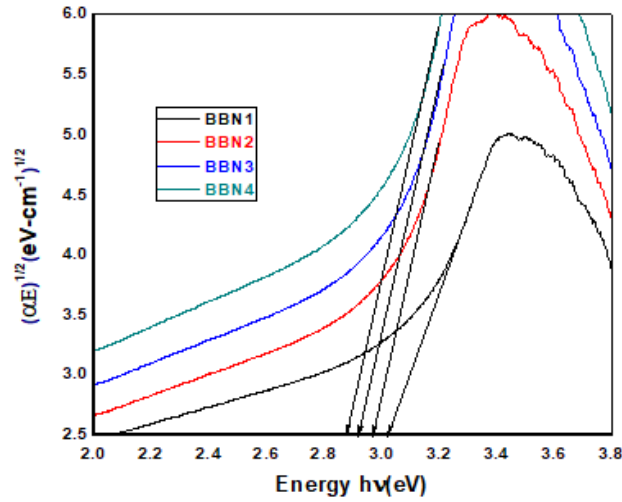


Figure 4. Tauc's plot for direct energy band gap of BBN glasses.



**Figure 5.** Tauc's plot for indirect energy band gap of BBN glasses.

Urbach's law, as follows, is applicable to the primary absorption edge at lower incident photon energy ( $h\nu$ ) and absorption coefficient  $\alpha(\nu)$ <sup>[25]</sup>.

$$\alpha(\nu) = C \cdot \exp\left(\frac{h\nu}{Eu}\right) \quad (12)$$

where  $\Delta E$  is the Urbach's energy and  $B$  is a constant. The slopes of the linear areas in the plots of  $\ln \alpha(\omega)$  vs.  $h\nu$  are used to get the values of Urbach energy. (**Figure 6** shows these curves for BBN glasses).

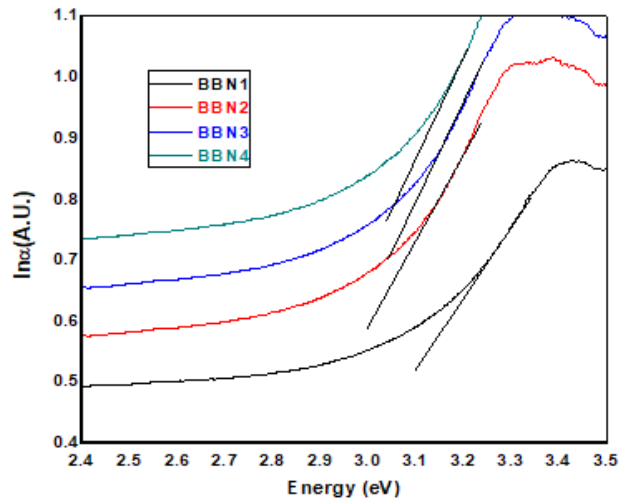


**Figure 6.** Plot between  $\ln \alpha$  and  $h\nu$  for Urbach energy of BBN glasses.

### 3.2.2. Refractive index

Using the relation established by, the refractive indices ( $n$ ) of the samples are calculated from the optical band gap values ( $E_{op}$ )<sup>[26-27]</sup>.

$$\frac{n^2-1}{n^2+1} = 1 - \sqrt{\frac{E_{op}^2}{20}} \quad (13)$$

**Table 2** provides the refractive index values that were determined using equation 13.

**Table 2.** Optical properties of BBN glasses.

Physical Properties	BBN1	BBN2	BBN3	BBN4
Direct forbidden energy gap( $E_{op}$ )(eV)	3.17	3.12	3.07	3.02
Indirect forbidden energy gap( $E_{op}$ )(eV)	2.84	2.862	2.884	2.905
Refractive index(RI)	2.006	2.016	2.026	2.036
Urbach's Energy $E_u$ (eV)	0.86280	0.693074	0.628607	0.617874

Refractive index values increased almost linearly within increase of bismuth oxides and optical band gaps and decreases. Variation in optical energy band gap and refractive index with share of bismuth oxide concentration are shown in **Figure 7**.

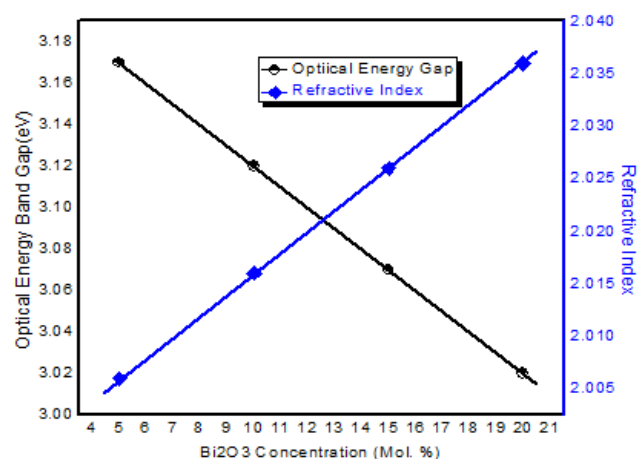


**Figure 7.** Variation in optical energy band gap and refractive index with change in the concentration of Bi<sub>2</sub>O<sub>3</sub>.

## 4. Conclusions

In summary, this means that research on the optical and physical characteristics of bismuth doped borate glasses yields a number of findings. It was found that as the concentration of Bi<sub>2</sub>O<sub>3</sub> increased, it also increased the molar volume and density. The noncrystalline character of the samples was validated by the XRD results. A decrease was observed in the internuclear distance, polaron radius, average distance between B-B atoms, and field intensity. The oxygen packing density dropped from 113.1876 to 75.29311. The Urbach's energy and steepness parameter were used to calculate the samples' disorderliness and is found in the range between 0.86280 eV to 0.617874 eV. The refractive index of BBN glasses is found in the range 2.006 to 2.036. Ultimately, this investigation demonstrated that the synthesised glasses' metallization criteria findings are optimal for nonlinear optical systems.

## Competing interests

The author declare no competing interests.

## References

1. Khattak GD, Tabet N, Wenger LE. Structural properties of glasses in the series ( Sr O ) x ( V 2 O 5 ) 1 - x , ( Sr O ) 0.5 - y ( B 2 O 3 ) y ( V 2 O 5 ) 0.5 , and ( Sr O ) 0.2 ( B 2 O 3 ) z ( V 2 O 5 ) 0.8 - z. Phys Rev B 2005;72:104203. <https://doi.org/10.1103/PhysRevB.72.104203>.
2. Murugavel S, Roling B. Ion transport mechanism in borate glasses: Influence of network structure on non-Arrhenius conductivity. Phys Rev B 2007; 76:180202. <https://doi.org/10.1103/PhysRevB.76.180202>.

3. Rajyasree Ch, Rao DK. Spectroscopic investigations on alkali earth bismuth borate glasses doped with CuO. *Journal of Non-Crystalline Solids* 2011; 357:836–41. <https://doi.org/10.1016/j.jnoncrysol.2010.11.008>.
4. Sharma G, Thind KS, Monika, Singh H, Manupriya, Gerward L. Optical properties of heavy metal oxide glasses before and after g - irradiation. *Physica Status Solidi (a)* 2007; 204:591–601. <https://doi.org/10.1002/pssa.200622124>.
5. Limkitjaroenporn P, Kaewkhao J, Tuscharoen S, Limsuwan P, Chewpraditkul W. Structural Studies of Lead Sodium Borate Glasses. *AMR* 2010; 93–94:439–42. <https://doi.org/10.4028/www.scientific.net/AMR.93-94.439>.
6. Dimitrov V, Sakka S. Electronic oxide polarizability and optical basicity of simple oxides. I. *Journal of Applied Physics* 1996; 79:1736–40. <https://doi.org/10.1063/1.360962>.
7. Ihara R, Benino Y, Fujiwara T, Komatsu T. Surface crystallization and second-order optical non-linearity in Gd<sub>2</sub>O<sub>3</sub>-Bi<sub>2</sub>O<sub>3</sub>-B<sub>2</sub>O<sub>3</sub> glasses. *Science and Technology of Advanced Materials* 2005; 6:138–42. <https://doi.org/10.1016/j.stam.2004.11.005>.
8. DeParis O, Mezzapesa FP, Corbari C, Kazansky PG, Sakaguchi K. Origin and enhancement of the second-order non-linear optical susceptibility induced in bismuth borate glasses by thermal poling. *Journal of Non-Crystalline Solids* 2005; 351:2166–77. <https://doi.org/10.1016/j.jnoncrysol.2005.06.004>.
9. Gomes ASL, Falcão Filho EL, De Araújo CB, Rativa D, De Araujo RE, Sakaguchi K, et al. Third-order nonlinear optical properties of bismuth-borate glasses measured by conventional and thermally managed eclipse Z scan. *Journal of Applied Physics* 2007; 101:033115. <https://doi.org/10.1063/1.2434940>.
10. Insitipong S, Kaewkhao J, Ratana T, Limsuwan P. Optical and structural investigation of bismuth borate glasses doped with dy<sup>3+</sup>. *Procedia Engineering* 2011; 8:195–9. <https://doi.org/10.1016/j.proeng.2011.03.036>.
11. Swapna K. Sk. Mahamuda, A. Srinivasa Rao, M. Jayasimhadri, T. Sasikala, L. Rama Moorthy. *J. Lumin.* 2013; 139:119.
12. Swapna K, MahamudaSk, Rao AS, Sasikala T, Packiyaraj P, Moorthy LR, et al. Luminescence characterization of Eu<sup>3+</sup> doped Zinc Alumino Bismuth Borate glasses for visible red emission applications. *Journal of Luminescence* 2014; 156:80–6. <https://doi.org/10.1016/j.jlumin.2014.07.022>.
13. Swapna K, MahamudaSk, Rao AS, Jayasimhadri M, Shakya S, Prakash GV. Tb<sup>3+</sup> doped Zinc Alumino Bismuth Borate glasses for green emitting luminescent devices. *Journal of Luminescence* 2014; 156:180–7. <https://doi.org/10.1016/j.jlumin.2014.08.019>.
14. Singla S, Achanta VG, Mahendru N, Prabhu SS, Falconieri M, Sharma G. High refractive index gold nanoparticle doped Bi<sub>2</sub>O<sub>3</sub>-B<sub>2</sub>O<sub>3</sub> glasses for THz frequencies. *Optical Materials* 2017; 72:91–7. <https://doi.org/10.1016/j.optmat.2017.05.043>.
15. Munisudhakar B, Nageswara Raju C, Reddi Babu M, Reddy NM, Rama Moorthy L. Luminescence characteristics of Nd<sup>3+</sup> doped bismuth borate glasses for photonic applications. *Materials Today: Proceedings* 2020; 26:5–10. <https://doi.org/10.1016/j.matpr.2019.05.349>.
16. Hall DW, Newhouse MA, Borrelli NF, Dumbaugh WH, Weidman DL. Nonlinear optical susceptibilities of high-index glasses. *Applied Physics Letters* 1989; 54:1293–5. <https://doi.org/10.1063/1.100697>.
17. Stehle C, Vira C, Hogan D, Feller S, Affatigato M. Optical and physical properties of bismuth borate glasses related to structure. *Physics and chemistry of glasses.* 1998 Apr 1; 39(2):83-6.
18. George HB, Vira C, Stehle C, Meyer J, Evers S, Hogan D, Feller S, Affatigato M. A structural analysis of the physical properties of bismuth and lead based glasses. *Physics and chemistry of glasses.* 1999 Dec 1; 40(6):326-32.
19. Terashima K, Shimoto TH, Yoko T. Structure and nonlinear optical properties of PbO-Bi<sub>2</sub>O<sub>3</sub>-B<sub>2</sub>O<sub>3</sub> glasses. *Physics and chemistry of glasses.* 1997; 38(4):211-7.
20. Ansari GF, Patidar S, Pandey R, Kumar R. Physical and Optical Properties of Lead-Tungsten-Tellurite Glasses. *MSF* 2023; 1097:71–6. <https://doi.org/10.4028/p-L9t2vI>.
21. Rezaul Karim S, Khan S, Ansari GF, Mishra D, Kumar S, Ashiq M. X-ray attenuation performance of a newly synthesized tellurium based lead-free radiation shielding glass system. *Radiation Physics and Chemistry* 2024; 216:111477. <https://doi.org/10.1016/j.radphyschem.2023.111477>.
22. Azuraida A, Halimah MK, Sidek AA, Azurahaman CA, Iskandar SM, Ishak M, Nurazlin A. Comparative studies of bismuth and barium boro-tellurite glass system: structural and optical properties. *Chalcogenide Lett.* 2015 Oct 1; 12(10):497-503.
23. Umar SA, Halimah MK, Chan KT, Latif AA. Physical, structural and optical properties of erbium doped rice husk silicate borotellurite (Er-doped RHSBT) glasses. *Journal of Non-Crystalline Solids* 2017; 472:31–8. <https://doi.org/10.1016/j.jnoncrysol.2017.07.013>.
24. Davis EA, Mott NF. Conduction in non-crystalline systems V. Conductivity, optical absorption and photoconductivity in amorphous semiconductors. *Philosophical Magazine* 1970; 22:0903–22. <https://doi.org/10.1080/14786437008221061>.
25. Urbach F. The long-wavelength edge of photographic sensitivity and of the electronic absorption of solids. *Physical review.* 1953 Dec 1; 92(5):1324.



26. Jat S, Sharma RK, Mahajan SK, Ashiq M, Ansari GF. Synthesis and optical properties of ternary TeO<sub>2</sub>-Bi<sub>2</sub>O<sub>3</sub>-Na<sub>2</sub>O glass system. *Materials Today: Proceedings* 2021; 42:1329–32.  
<https://doi.org/10.1016/j.matpr.2020.12.1188>.
27. Fares H, Elhouichet H, Gelloz B, Férid M. Silver nanoparticles enhanced luminescence properties of Er<sup>3+</sup> doped tellurite glasses: Effect of heat treatment. *Journal of Applied Physics* 2014; 116:123504.  
<https://doi.org/10.1063/1.4896363>.